New Journal of Physics
The open access journal at the forefront of physics

Deutsche Physikalische Gesellschaft DPG IOP Institute of Physics

PAPER • OPEN ACCESS

Discriminatory resonance energy transfer mediated by a chiral environment

To cite this article: Janine C Franz *et al* 2024 *New J. Phys.* **26** 053002

IOP Publishing New J. Phys. 26 (2024) 053002 https://doi.org/10.1088/1367-2630/ad3f9c

New Journal of Physics
The open access journal at the forefront of physics

Deutsche Physikalische Gesellschaft DPG
IOP Institute of Physics

Published in partnership with: Deutsche Physikalische Gesellschaft and the Institute of Physics

OPEN ACCESS

RECEIVED
22 January 2024

REVISED
10 April 2024

ACCEPTED FOR PUBLICATION
16 April 2024

PUBLISHED
7 May 2024

PAPER

Discriminatory resonance energy transfer mediated by a chiral environment

Janine C Franz[1,*], **Stefan Yoshi Buhmann**[1,*] **and A Salam**[2,*]

[1] Institut für Physik, Universität Kassel, Kassel, 34132, Germany
[2] Department of Chemistry, Wake Forest University, Winston-Salem, NC, 27109, United States of America
[*] Authors to whom any correspondence should be addressed.

E-mail: janine.franz@uni-kassel.de, stefan.buhmann@uni-kassel.de and salama@wfu.edu

Keywords: chiral, energy transfer, RET, environment, macroscopic medium, macroscopic QED, discrimination

Abstract

In this study, we delve into the crucial influence of and enhancement by chiral environments on the discriminatory capabilities of resonance energy transfer. Firstly, we scrutinize the impact of a macroscopic chiral medium enveloping the interacting molecules; secondly, we probe the effect of a chiral mediating molecule in close proximity to the system. Importantly, our findings demonstrate that chiral environments not only modulate pre-existing discriminatory effects but also introduce novel mechanisms for discrimination. Central to our research is the application of an innovative model for chiral local-field corrections, which unveils a remarkable distance-dependent inversion of the discrimination dynamics. Our study extends beyond the confines of any specific molecular system, offering a comprehensive discussion of these diverse effects, thereby providing insights with broader implications. Finally, we present a comparative analysis across all studied systems, illustrating our insights by employing 3-methyl-cyclopentanone as an example molecule.

1. Introduction

Resonance energy transfer (RET) involving chiral molecules can in principle be used to discriminate between differently handed acceptors [1–3]. In this process, the energy of an initially excited donor particle is transferred via the electromagnetic field to a ground-state acceptor particle [4, 5]. Considering a chiral donor molecule with known handedness, one can predict that the energy transfer rate occurring between same-handed molecular pairs is larger than the one between opposite-handed ones and hence use this difference to distinguish the chiral acceptor [1].

In free space, the relative difference between the rates of these two scenarios, i.e. the degree of discrimination, is quite small and proportional to the product of the molecular rotatory strengths [6]. It has been shown that immersing the considered system inside a dielectric medium can modify and enhance the discriminatory effect of RET [1]. Such a situation provides an early example in the emerging sub-field of chiral polaritonics [7–9].

Here, we consider the impact of a chiral environment on the degree of discrimination via RET. Chiral matter has been well-established to interact fundamentally differently with the electromagnetic field when compared to nonchiral counterparts, leading to intriguing implications for light-matter interactions [10, 11]. We find two different effects: the chiral environment modifies the degree of discrimination that is originally found in free space and, assuming the handedness of the chiral environment is known, the environment itself can actively discriminate the acceptors. The latter constitutes a new discriminatory effect that survives even when considering nonchiral donor molecules and is entirely due to the chiral properties of the environment itself. It is important to point out that RET is not the only elementary coupling process between optically active particles of matter that exhibits discrimination. The van-der-Waals dispersion energy shift between a pair of chiral molecules is also discriminatory, and has been calculated within the frameworks of microscopic and macroscopic quantum electrodynamic (QED) [12–14].

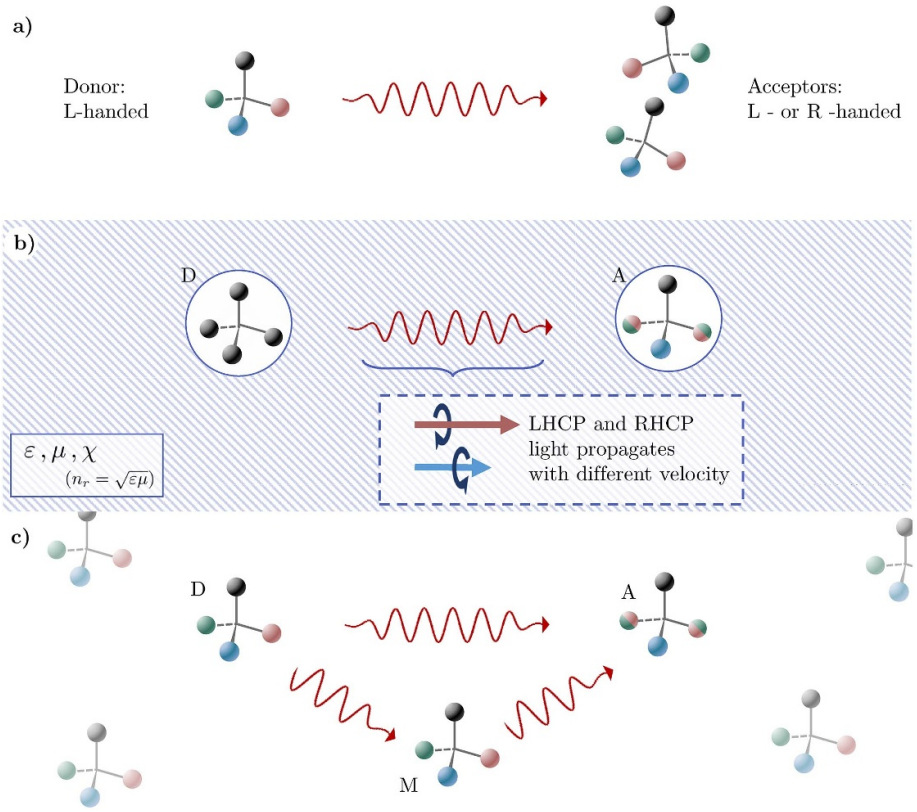

Figure 1. Schemes of the three different scenarios considered in this paper. (a) For comparison, and as a simple introductory example, we first consider the discrimination via RET in free space where the handedness of the donor is known, e.g. to be left-handed and the acceptor can have either handedness. (b) Secondly, we study the discrimination with an additional chiral medium surrounding the system where we include local-field corrections and assume that the medium is known to be same-handed as the donor. (c) Lastly, we consider the discrimination in the presence of a single chiral mediator molecule with known handedness as an approximation in the limit of a dilute gas surrounding the system.

While the initial attention of chiral discrimination focussed on interactions between optically active systems, for example in dispersion forces and absorption/emission processes, recent work has explored sensing and separation techniques involving three-wave mixing in the microwave region, enantio-specific population transfer in few-level systems, photo-electron circular dichroism, and high-harmonic generation, most commonly treated solely within the electric dipole approximation [15–19]. Environmental effects are also expected to play a significant role in these newer processes, especially if the medium is chiral or if a chiral molecule is in close proximity to the photoactive centre. Processes that rely on the optical activity of the molecule may be expected to behave qualitatively similar to the cases discussed in this work while the environmental impact on solely electrical processes are expected to be fundamentally different.

We start by discussing the discrimination of the acceptor molecule via RET in free space as an introductory case as well as for comparison. We then consider the donor–acceptor pair first immersed inside a chiral medium with known handedness. In the limit of a very dilute gas the surrounding medium is rather modelled by its individual constituents [20–27]. We therefore consider lastly the discrimination in the presence of a single additional chiral molecule [28], called mediator. The three scenarios discussed in this paper are schematically shown in figure 1.

To be able to consider a chiral medium which the molecules are immersed in, we have derived the local-field corrections (LFC) to account for local-field and screening effects inside chiral media based on the Onsager real cavity model [29]. The results show a surprising effect on the discrimination where the LFCs lead to an inversion of the discrimination as a function of the intermolecular distance. We account for the chiral mediator as part of the environment within the framework of macroscopic QED [30–32], by extending the known method for electric particles [33] to optically active molecules [14, 34].

We present the results analytically for the limits of small and large intermolecular distance, as well as discuss general results in the form of plots for the total distance regime. As a summary, we illustrate the degree of discrimination for all discussed cases for 3-methyl-cyclopentanone chosen as the example chiral molecules.

2. Discriminatory RET rate

The presented results are obtained from purely analytic calculations within the framework of macroscopic QED. The process of RET is described via perturbation theory, leading to Fermi's golden rule in second order for the calculation of the RET rate. The resulting rate expression can ultimately be separated into discriminatory and nondiscriminatory rate contributions in each of the three considered scenarios, see figure 1.

We consider the interaction of chiral molecules with each other via the electromagnetic field. Because we assume each molecule to be optically active, we account for the coupling of the magnetic dipole to the magnetic field, $\hat{\boldsymbol{B}}$, as well as the usual interaction of the electric dipole to the electric field, $\hat{\boldsymbol{E}}$, as expressed in the interaction Hamiltonian [35]

$$\hat{H}_{\mathrm{int}} = -\sum_{\alpha=\mathrm{D,A}} \left[\hat{\boldsymbol{d}}^{(\alpha)} \cdot \hat{\boldsymbol{E}}(\boldsymbol{r}_\alpha) + \hat{\boldsymbol{m}}^{(\alpha)} \cdot \hat{\boldsymbol{B}}(\boldsymbol{r}_\alpha) \right], \tag{1}$$

where $\boldsymbol{r}_{\mathrm{D/A}}$ is the donor's/acceptor's position, $\hat{\boldsymbol{d}}^{\mathrm{D/A}}$ is the donor's/acceptor's electric dipole moment operator and $\hat{\boldsymbol{m}}^{\mathrm{D/A}}$ is its magnetic counterpart. In this order of multipole expansion, the electric quadrupole usually needs to be considered as well. However, in this work we are interested in the rates between molecules with arbitrary orientation, leading to isotropic averaging. In this situation the contribution to the rate due to the interference of electric dipole and quadrupole moments is known to vanish [2].

The process rate Γ of RET, where the excitation is transferred from the donor to the acceptor, can then be derived via Fermi's golden rule, such that

$$\Gamma = \frac{2\pi}{\hbar^2} \rho\left(\omega_f\right) |M_{fi}|^2 , \tag{2}$$

where $\rho(\omega_f)$ is the spectral overlap between the donor's emission and the acceptor's absorption spectrum at the energy of the final state $\hbar\omega_f$ [36–38], and M_{fi} is here the second order transition matrix element, whose computation relies on the initial and final states of the system as well as the interaction Hamiltonian,

$$M_{fi} = \sum_j \frac{\langle f|\hat{H}_{\mathrm{int}}|j\rangle \langle j|\hat{H}_{\mathrm{int}}|i\rangle}{E_i - E_j}\bigg|_{E_i = E_f} , \tag{3}$$

where we sum over all intermediate states $|j\rangle$, while $|i\rangle$, $|f\rangle$ label the initial and final state respectively and E_n is the energy of the respective state $|n\rangle$. The initial and final states are given by product matter–field states, $|i\rangle = |1\rangle_{\mathrm{D}}|0\rangle_{\mathrm{A}}|\{0\}\rangle_F$ and $|f\rangle = |0\rangle_{\mathrm{D}}|1\rangle_{\mathrm{A}}|\{0\}\rangle_F$, where $|0/1\rangle_{\mathrm{A/D}}$ labels the ground/excited state of the acceptor/donor and $|\{0\}\rangle_F$ denotes the ground state of the electromagnetic field. The intermediate states $|j\rangle$ are of two types and correspond either to both molecules in the ground state or both in the excited state, with one virtual photon (polariton) present in each case. Explicitly,

$$|j\rangle \in \left\{ |0\rangle_{\mathrm{D}}|0\rangle_{\mathrm{A}}|\mathbf{1}_{\mathrm{e/m}}(\boldsymbol{r},\omega)\rangle_F , |1\rangle_{\mathrm{D}}|1\rangle_{\mathrm{A}}|\mathbf{1}_{\mathrm{e/m}}(\boldsymbol{r},\omega)\rangle_F \,\middle|\, \forall\omega > 0 , \forall \boldsymbol{r} \in \mathbb{R}^3 \right\} , \tag{4}$$

where $|\mathbf{1}_{\mathrm{e/m}}(\boldsymbol{r},\omega)\rangle_F$ is an electric/magnetic body-field excitation with energy $\hbar\omega$ at position $\boldsymbol{r}$.

It was shown that within the framework of macroscopic QED this leads to the RET rate [1]

$$\Gamma = \sum_{\lambda_1,\lambda_2,\lambda_3,\lambda_4} \Gamma_{\lambda_1\lambda_2\lambda_3\lambda_4} , \tag{5}$$

$$\Gamma_{\lambda_1\lambda_2\lambda_3\lambda_4} = \frac{2\pi\rho\mu_0^2}{9\hbar^2} \left(\boldsymbol{d}^{\mathrm{A}}_{\lambda_1} \cdot \boldsymbol{d}^{\mathrm{A}*}_{\lambda_2} \right) \left(\boldsymbol{d}^{\mathrm{D}*}_{\lambda_3} \cdot \boldsymbol{d}^{\mathrm{D}}_{\lambda_4} \right) \mathrm{Tr}\left[\mathbb{G}_{\lambda_1\lambda_4} \cdot \mathbb{G}^{*T}_{\lambda_2\lambda_3} \right] , \tag{6}$$

where we have assumed that the relative orientation of the molecules is isotropic, such that $\boldsymbol{d}_1 \otimes \boldsymbol{d}_2 = (\boldsymbol{d}_1 \cdot \boldsymbol{d}_2)\mathbb{I}/3$, and we adopted a dual formulation with $\lambda_i \in \{\mathrm{e},\mathrm{m}\}$ that is useful when considering the duality symmetry of electric and magnetic fields in the absence of free charges [33]. The dual transition dipoles are given by

$$\boldsymbol{d}^{\mathrm{A}}_{\mathrm{e}} = \langle 1|\hat{\boldsymbol{d}}|0\rangle_{\mathrm{A}} , \qquad \boldsymbol{d}^{\mathrm{D}}_{\mathrm{e}} = \langle 0|\hat{\boldsymbol{d}}|1\rangle_{\mathrm{D}} , \tag{7}$$

$$\boldsymbol{d}^{\mathrm{A}}_{\mathrm{m}} = \frac{\langle 1|\hat{\boldsymbol{m}}|0\rangle_{\mathrm{A}}}{c} , \qquad \boldsymbol{d}^{\mathrm{D}}_{\mathrm{m}} = \frac{\langle 0|\hat{\boldsymbol{m}}|1\rangle_{\mathrm{D}}}{c} , \tag{8}$$

where the transition dipoles of the donor correspond to a downward transition and the ones of the acceptor to an upward one. The dual Green's tensor is given by

$$\mathbb{G}_{\lambda\lambda'} = \begin{cases} \frac{\mathrm{i}\omega}{c}\mathbb{G}(\boldsymbol{r}_\mathrm{A},\boldsymbol{r}_\mathrm{D},\omega)\frac{\mathrm{i}\omega}{c}, & \text{for } \lambda\lambda' = \mathrm{ee} \\ \overrightarrow{\nabla}_\mathrm{A}\times\mathbb{G}(\boldsymbol{r}_\mathrm{A},\boldsymbol{r}_\mathrm{D},\omega)\times\overleftarrow{\nabla}_\mathrm{D}, & \text{for } \lambda\lambda' = \mathrm{mm} \\ \frac{\mathrm{i}\omega}{c}\mathbb{G}(\boldsymbol{r}_\mathrm{A},\boldsymbol{r}_\mathrm{D},\omega)\times\overleftarrow{\nabla}_\mathrm{D}, & \text{for } \lambda\lambda' = \mathrm{em} \\ \overrightarrow{\nabla}_\mathrm{A}\times\mathbb{G}(\boldsymbol{r}_\mathrm{A},\boldsymbol{r}_\mathrm{D},\omega)\frac{\mathrm{i}\omega}{c}, & \text{for } \lambda\lambda' = \mathrm{me} \end{cases} \tag{9}$$

where $\hbar\omega = \hbar\omega^\mathrm{D} = \hbar\omega^\mathrm{A}$ is the transition energy and the arrow on the nabla-operator indicates in which direction the derivative acts. The Green's tensor $\mathbb{G}$ can reflect the influence of the surrounding macroscopic environment by solving the Helmholtz equation for the respective environment and its boundary conditions.

The isotropic RET rate (5) features the scalar product of the different transition dipoles involved in the migration of energy. The scalar product between electric and magnetic transition dipole moments is related to the so-called optical rotatory strength R of the respective chiral molecule,

$$R = \mathrm{Im}\left[c\langle 0|\hat{\boldsymbol{d}}_\mathrm{e}|1\rangle\cdot\langle 1|\hat{\boldsymbol{d}}_\mathrm{m}|0\rangle\right], \tag{10}$$

and its sign depends on the molecule's handedness. In our notational convention, where $\boldsymbol{d}_\lambda^\mathrm{D}$ denotes a downward transition, while $\boldsymbol{d}_\lambda^\mathrm{A}$ represents an upward transition, the respective rotatory strengths are given by

$$R_\mathrm{D} = \mathrm{Im}\left[c\boldsymbol{d}_\mathrm{e}^\mathrm{D}\cdot\boldsymbol{d}_\mathrm{m}^{\mathrm{D}*}\right], \qquad R_\mathrm{A} = \mathrm{Im}\left[c\boldsymbol{d}_\mathrm{e}^{\mathrm{A}*}\cdot\boldsymbol{d}_\mathrm{m}^\mathrm{A}\right]. \tag{11}$$

The total RET rate Γ then features a contribution whose overall sign is sensitive to the acceptor's handedness and one that is insensitive. We refer to the former as the discriminatory rate contribution Γ_disc, the latter as the non-discriminatory one Γ_nd, and the rates Γ_L and Γ_R involving left- and right-handed acceptors, respectively, differ by $2\Gamma_\mathrm{disc}$. This leads to the definition of the degree of discrimination δ as

$$\delta = \frac{\Gamma_\mathrm{L}-\Gamma_\mathrm{R}}{\Gamma_\mathrm{L}+\Gamma_\mathrm{R}} = \frac{\Gamma_\mathrm{disc}}{\Gamma_\mathrm{nd}}. \tag{12}$$

By definition δ can range from negative unity to unity, where for positive values left-handed acceptors are preferred by the energy transfer $\Gamma_\mathrm{L} > \Gamma_\mathrm{R}$, and vice versa for negative ones. Unity values, $\delta = \pm 1$ then correspond to perfect discrimination, where no energy transfer occurs to one of the enantiomers. For simplicity, and without loss of generality we assume henceforth that the donor is known to be left-handed. The analogous results for opposite-handed donors can then be obtained by swapping the respective left- and right-handed labels.

In accordance with the Curie symmetry principle, we find that the discriminatory rate contribution depends on the product of the chiral property of the acceptor and another chiral object, and thus only on their relative handedness. In free space, this additional chiral object is the donor molecule. The chiral property of the molecules appearing in the rate is the rotatory strength of the acceptor R_A and the donor R_D, defined by equation (11), i.e. $\Gamma_\mathrm{disc} \propto R_\mathrm{A}R_\mathrm{D}$. Introducing additional chiral objects with a predetermined handedness into the system then results in supplementary discriminatory rate contributions, which depend on the chirality of these objects.

3. Accounting for the effect of a chiral environment

We want to analyse the influence on the discriminatory effect of RET by additional chiral objects in the environment. Here, we briefly introduce the two environments considered, a surrounding chiral medium and a single chiral mediator molecule, and how they can be treated within the framework of macroscopic QED via their appropriate Green's tensor.

3.1. Green's tensor for chiral medium with LFC

In a chiral medium magnetic and electric fields are coupled to each other via the macroscopic constitutive relations:

$$\hat{\boldsymbol{D}} = \varepsilon\varepsilon_0\hat{\boldsymbol{E}} + \hat{\boldsymbol{P}}_N - \mathrm{i}\frac{\chi}{c}\hat{\boldsymbol{H}} - \mathrm{i}\frac{\chi}{c}\hat{\boldsymbol{M}}_N, \tag{13}$$

$$\hat{\boldsymbol{B}} = \mu\mu_0\hat{\boldsymbol{H}} + \mu\mu_0\hat{\boldsymbol{M}}_N + \mathrm{i}\frac{\chi}{c}\hat{\boldsymbol{E}}, \tag{14}$$

where χ is the chiral parameter of the medium. In such a medium left- and right-handed circularly polarised (L- and R-HCP) light propagate with different wave numbers $k_{-/+} = (n_r \mp \chi)\omega/c$, where $-/+$ and

upper/lower signs refer to L- and R-HCP, respectively. As a consequence, the chiral bulk Green's tensor $\mathbb{G}^{\mathrm{c}}_{\lambda\lambda'}$ has a more complex structure than the magnetodielectric bulk one when expressed in a basis of wave vector functions, namely [39]

$$\mathbb{G}^{\mathrm{c}} = \mathbb{G}^{\mathrm{L}}(k_-) + \mathbb{G}^{\mathrm{R}}(k_+)\,, \tag{15}$$

$$\mathbb{G}^{\mathrm{L}}(k_-) = \frac{3\mathrm{i}\mu c}{8\pi\, n_c \omega} \sum_{\sigma,m\leqslant 1} k_-^2 \boldsymbol{L}^{(1)}_{\sigma m1}(\boldsymbol{r}, k_-) \otimes \boldsymbol{L}_{\sigma m1}(0, k_-)\,, \tag{16}$$

$$\mathbb{G}^{\mathrm{R}}(k_+) = \frac{3\mathrm{i}\mu c}{8\pi\, n_c \omega} \sum_{\sigma,m\leqslant 1} k_+^2 \boldsymbol{R}^{(1)}_{\sigma m1}(\boldsymbol{r}, k_+) \otimes \boldsymbol{R}_{\sigma m1}(0, k_+)\,, \tag{17}$$

where $\sigma \in \{\mathrm{g}, \mathrm{u}\}$ denote even or odd wave vector functions, $\mathbb{G}^{\mathrm{L/R}}$ describe the propagation of L/R-HCP excitations, $\boldsymbol{L}_{\sigma mn}/\boldsymbol{R}_{\sigma mn}$ are the spherical wave vector functions for L/R-HCP waves and we chose the source point to sit at the origin without loss of generality to simplify the expression.

The spherical wave vector functions can be defined by means of the electric and magnetic spherical vector harmonics $\boldsymbol{N}_{\sigma mn}$ and $\boldsymbol{M}_{\sigma mn}$ as [39]

$$\boldsymbol{L}_{\sigma mn}(\boldsymbol{r}, k) = \frac{\boldsymbol{N}_{\sigma mn}(\boldsymbol{r}, k) + \boldsymbol{M}_{\sigma mn}(\boldsymbol{r}, k)}{\sqrt{2}}\,, \tag{18}$$

$$\boldsymbol{R}_{\sigma mn}(\boldsymbol{r}, k) = \frac{\boldsymbol{N}_{\sigma mn}(\boldsymbol{r}, k) - \boldsymbol{M}_{\sigma mn}(\boldsymbol{r}, k)}{\sqrt{2}}\,. \tag{19}$$

The additional superscript (1) in equations (16) and (17) denotes the replacement of spherical Bessel functions by Hankel functions within the definitions of $\boldsymbol{M}$ and $\boldsymbol{N}$ and represents ingoing and outgoing waves, respectively. The basis set $\boldsymbol{L}_{\sigma mn}$ and $\boldsymbol{R}_{\sigma mn}$ are then eigenvectors of the helicity operator $\hat{\Lambda} = \hat{\boldsymbol{p}}/|\hat{\boldsymbol{p}}|\times$ where $\hat{\boldsymbol{p}}$ is the momentum operator, with eigenvalues $\lambda_{\mp} = \mp 1$. Note that there are different conventions in which polarisation is considered left- and right-handed.

Assuming small chirality of the medium, $\chi \ll 1$, the bulk Green's tensor can then be approximated by

$$\begin{aligned}\mathbb{G}^{(0)} = {} & \frac{\mu e^{\mathrm{i}n_r k_0 r}}{4\pi\, k_0^2 n_r^2 r^3}\left[\left(n_r^2 k_0^2 r^2 + i n_r k_0 r - 1\right)\mathbb{I} - \left(n_r^2 k_0^2 r^2 + 3 i n_r k_0 r - 3\right)\boldsymbol{e}_r \otimes \boldsymbol{e}_r\right] \\ & + \chi \frac{\mu k_0 e^{\mathrm{i}n_r k_0 r}}{4\pi}\left[\boldsymbol{e}_\phi \otimes \boldsymbol{e}_\theta - \boldsymbol{e}_\theta \otimes \boldsymbol{e}_\phi\right],\end{aligned} \tag{20}$$

where $k_0 = \omega/c$ is the vacuum wave number and $\boldsymbol{e}_r$, $\boldsymbol{e}_\theta$ and $\boldsymbol{e}_\phi$ are the spherical unit vectors of $\boldsymbol{r} = \boldsymbol{r}_{\mathrm{D}} - \boldsymbol{r}_{\mathrm{A}}$.

When modelling atomic or molecular interactions inside a surrounding macroscopic medium, local-field and screening effects need to be taken into account. This can be achieved by using LFC models. Here, we choose the Onsager real cavity model [29] to work out the corrections due to local-field effects inside a chiral medium. In a nonchiral medium, this leads to correction factors to the total Green's tensor that differ for electric and magnetic interactions. In a chiral medium, we find that additionally to the distinction of magnetic and electric interactions, L- and R-HCP excitations need to be corrected via different factors as well. The corrected dual Green's tensor is then given by

$$\mathbb{G}^{\mathrm{c,lfc}}_{\lambda\lambda'} = c_{\lambda\mathrm{L}} c_{\lambda'\mathrm{L}} \mathbb{G}^{\mathrm{L}}_{\lambda\lambda'}(k_-) + c_{\lambda\mathrm{R}} c_{\lambda'\mathrm{R}} \mathbb{G}^{\mathrm{R}}_{\lambda\lambda'}(k_+)\,, \tag{21}$$

where the subscripts $\lambda, \lambda' \in \{\mathrm{e}, \mathrm{m}\}$ denote the additional factors and operations on the Green's tensor defined by equation (9) and the chiral correction factors are given by

$$c_{\mathrm{e}\frac{\mathrm{L}}{\mathrm{R}}} = \frac{3\,(n_r \mp \chi)\,(\pm 2\mu\chi + 2\mu n_r + n_r)}{\mu\,(2\mu - 4\chi^2 + 1) + n_r^2\,(4\mu + 2)}\,, \tag{22}$$

$$c_{\mathrm{m}\frac{\mathrm{L}}{\mathrm{R}}} = \frac{3\left(\mu + 2n_r^2 \pm 2n_r\chi\right)}{\mu\,(2\mu - 4\chi^2 + 1) + n_r^2\,(4\mu + 2)}\,. \tag{23}$$

In the limit of small χ, we can write them as

$$c_{\mathrm{eL}} \approx c_{\mathrm{e}} - \chi\zeta_{\mathrm{e}}\,, \qquad c_{\mathrm{eR}} \approx c_{\mathrm{e}} + \chi\zeta_{\mathrm{e}}\,, \tag{24}$$

$$c_{\mathrm{mL}} \approx c_{\mathrm{m}} + \chi\zeta_{\mathrm{m}}\,, \quad c_{\mathrm{mR}} \approx c_{\mathrm{m}} - \chi\zeta_{\mathrm{m}}\,, \tag{25}$$

where c_{e} and c_{m} are the well-known LFC factors for nonchiral media,

$$c_{\mathrm{e}} = \frac{3\varepsilon}{1 + 2\varepsilon}\,, \quad c_{\mathrm{m}} = \frac{3}{1 + 2\mu}\,, \tag{26}$$

and ζ_{e} and ζ_{m} are given by

$$\zeta_{\mathrm{e}} = \frac{c_{\mathrm{e}} c_{\mathrm{m}}}{3 n_r}, \quad \zeta_{\mathrm{m}} = \frac{2 c_{\mathrm{e}} c_{\mathrm{m}}}{3 n_r}. \tag{27}$$

The introduction of different correction factors for left- and right-handed circularly polarised waves alters the structure of the Green's tensor significantly more than in the nonchiral case, where LFC yields a mere overall scaling of the total Green's tensor.

3.2. Green's tensor for chiral mediator

In the limit of dilute gases the surrounding medium can be modelled by N mediator molecules. Electric mediators can be viewed as an environment by explicitly including them in the Green's tensor via their electric polarisability [20–22, 40]. Here, we extend the theory to chiral mediator molecules in the environment. The considered system is schematically shown in figure 1(c). We consider only a single mediator moelcule here and analyse the geometry dependent discrimination in such a system. The generalisation to a density of mediators, donors and acceptors is then straightforward, where in case of several donors one has to distinguish between coherent and incoherent initial states of the donor molecules. We assume that the mediator itself is a chiral molecule in its ground state that features a resonance at the exchanged energy $\hbar\omega$. Additionally, we assume that the transitions of the mediator molecule are isotropic and that the intermolecular distances are larger than their size, such that we may approximate the mediator as point-like but still retain the dipole approximation. Finally, assuming that the dilute-gas limit of the Clausius-Mosotti relation is a good approximation, we find for the dual Green's tensor,

$$\mathbb{G}_{\lambda_1\lambda_2}(\boldsymbol{r}_{\mathrm{A}}, \boldsymbol{r}_D) = \mathbb{G}^{(0)}_{\lambda_1\lambda_2}(\boldsymbol{r}_{\mathrm{A}}, \boldsymbol{r}_D) + \mathbb{G}^{\mathrm{M}}_{\lambda_1\lambda_2}(\boldsymbol{r}_{\mathrm{A}}, \boldsymbol{r}_D), \tag{28}$$

$$\mathbb{G}^{\mathrm{M}}_{\lambda_1\lambda_2}(\boldsymbol{r}_{\mathrm{A}}, \boldsymbol{r}_D) = -\sum_{\lambda,\lambda'} \mathbb{G}^{(0)}_{\lambda_1\lambda}(\boldsymbol{r}_{\mathrm{A}}, \boldsymbol{r}_{\mathrm{M}}) \cdot \frac{\boldsymbol{\alpha}_{\lambda\lambda'}}{\varepsilon_0} \cdot \mathbb{G}^{(0)}_{\lambda'\lambda_2}(\boldsymbol{r}_{\mathrm{M}}, \boldsymbol{r}_{\mathrm{D}}), \tag{29}$$

where $\mathbb{G}^{(0)}_{\lambda\lambda'}$ is the dual free-space Green's tensor defined by equation (9) where $\mathbb{G}$ is substituted by the free-space Green's tensor $\mathbb{G}^{(0)}$ and $\boldsymbol{\alpha}_{\lambda\lambda'} = \boldsymbol{\alpha}_{\lambda\lambda'}(\omega_{\mathrm{D}})$ is the dual polarisability tensor of the mediator at ω_{D} given by

$$\boldsymbol{\alpha}_{\lambda\lambda'}(\omega_{\mathrm{D}}) = \frac{1}{3\hbar} \sum_k \left(\frac{\langle 0|\boldsymbol{d}_\lambda|k\rangle_{\mathrm{M}} \otimes \langle k|\boldsymbol{d}_{\lambda'}|0\rangle_{\mathrm{M}}}{\omega_k + \omega_{\mathrm{D}} + \mathrm{i}\gamma_k} + \frac{\langle k|\boldsymbol{d}_\lambda|0\rangle_{\mathrm{M}} \otimes \langle 0|\boldsymbol{d}_{\lambda'}|k\rangle_{\mathrm{M}}}{\omega_k - \omega_{\mathrm{D}} + \mathrm{i}\gamma_k} \right), \tag{30}$$

where $|k\rangle_{\mathrm{M}}$ are the excited states of M, ω_k are their transition frequencies and $1/\gamma_k$ the respective lifetimes. The chiral property of the mediator, i.e. its rotatory strength R_{M}, see equation (10), appears in the mixed electric-magnetic polarisabilities,

$$\boldsymbol{\alpha}_{\mathrm{em}} = -\boldsymbol{\alpha}^T_{\mathrm{me}} \propto R_{\mathrm{M}}. \tag{31}$$

Next, we apply some assumptions for the mediator to simplify the polarisability tensor. Assuming that there exists an excited state of M in resonance with ω_{D}, such that $\omega_k = \omega_{\mathrm{D}}$, we find that this resonance dominates $\alpha_{\lambda\lambda'}$. If we additionally assume that this resonant state is degenerate in its orbital magnetic quantum number, i.e. features an isotropic transition, we find that the polarisabilty tensor is proportional to the identity, $\boldsymbol{\alpha}_{\lambda\lambda'} = \alpha_{\lambda\lambda'}\mathbb{I}$ and given by

$$\alpha_{\lambda\lambda'} = \frac{1}{3\hbar} \left(\frac{\boldsymbol{d}^{\mathrm{M}}_\lambda \cdot \boldsymbol{d}^{\mathrm{M}*}_{\lambda'}}{2\omega + \mathrm{i}\gamma_{\mathrm{M}}} - \mathrm{i}\frac{\boldsymbol{d}^{\mathrm{M}}_{\lambda'} \cdot \boldsymbol{d}^{\mathrm{M}*}_{\lambda}}{\gamma_{\mathrm{M}}} \right), \tag{32}$$

where $\boldsymbol{d}^{\mathrm{M}}_\lambda = \langle 0|\hat{\boldsymbol{d}}_\lambda|1\rangle$ is the electric/magnetic transition dipole and γ_{M} is the linewidth of the resonant mediator transition. Assuming that there are no additional line-broadening effects, the linewidth is given by the spontaneous decay rate of the excited state, $\gamma_{\mathrm{M}} = \sum_\lambda \omega^3 |\boldsymbol{d}^{\mathrm{M}}_\lambda|^2/(3c^3\pi\varepsilon_0\hbar)$. The decay rate γ_{M} is much smaller than the eigenfrequency ω and hence $\mathrm{Re}\alpha_{\lambda\lambda'} \ll \mathrm{Im}\alpha_{\lambda\lambda'}$.

The theory can easily be extended to N mediators by introducing a sum over several M_i in equation (28) with their respective mediator Green's tensor $G^{\mathrm{M}_i}_{\lambda\lambda'}$. Even densities of identical mediators can be considered by replacing this sum with an integral over said density. Relaxing the assumption of isotropic transitions in the mediator molecule leads to off-diagonal components of the polarisability tensor and hence to additional contributions to $\mathbb{G}^{\mathrm{M}}$. It is plausible to assume that in many cases the contribution due to the diagonal of the α-tensor dominates and we restrict ourselves to isotropic transitions here to simplify the resulting discussion. Extending the framework to non-isotropic transitions is however straightforward.

4. RET rate expressions

Here, we provide explicit analytical expressions for the derived and studied rates.

4.1. RET rate in vacuum

In vacuum we use the free-space Green's tensor to evaluate the rate formula (5). It is given by

$$\mathbb{G}^{(0)}(\boldsymbol{r}_\mathrm{A},\boldsymbol{r}_\mathrm{D},\omega)=-\frac{c^2\mathrm{e}^{\mathrm{i}\omega r/c}}{4\pi\omega r^2}\left\{\left[1-\mathrm{i}\frac{\omega r}{c}-\frac{\omega^2 r^2}{c^2}\right]\mathbb{I}-\left[3-3\mathrm{i}\frac{\omega r}{c}-\frac{\omega^2 r^2}{c^2}\right]\boldsymbol{e}_r\otimes\boldsymbol{e}_r\right\}, \tag{33}$$

where $r=|\boldsymbol{r}_\mathrm{A}-\boldsymbol{r}_\mathrm{D}|$, $\mathbb{I}$ is the 3x3-identity matrix and $\boldsymbol{e}_r=(\boldsymbol{r}_\mathrm{A}-\boldsymbol{r}_\mathrm{D})/r$ is again the unit vector pointing from r_D to r_A. The discriminatory and nondiscriminatory contributions to the free space rate in terms of dual rate terms (6) are given by

$$\Gamma^0_\mathrm{disc}=\Gamma_\mathrm{emme}+\Gamma_\mathrm{emem}+\Gamma_\mathrm{meme}+\Gamma_\mathrm{meem}\propto R_\mathrm{A}R_\mathrm{D} \tag{34}$$

and

$$\Gamma^0_\mathrm{nd}=\sum_{\lambda\lambda'}\Gamma_{\lambda\lambda\lambda'\lambda'}. \tag{35}$$

Explicitly these expressions yield

$$\Gamma^0_\mathrm{disc}=\frac{\mu_0^2\rho R_\mathrm{D}R_\mathrm{A}}{18\pi\hbar^2 r^6}\left(3+2\frac{r^2\omega^2}{c^2}+2\frac{r^4\omega^4}{c^4}\right), \tag{36}$$

$$\begin{aligned}\Gamma^0_\mathrm{nd}=\frac{\mu_0^2\rho}{36\pi\hbar^2 r^6}\Bigg\{&3\left(|\boldsymbol{d}^\mathrm{A}_\mathrm{e}|^2|\boldsymbol{d}^\mathrm{D}_\mathrm{e}|^2+|\boldsymbol{d}^\mathrm{A}_\mathrm{m}|^2|\boldsymbol{d}^\mathrm{D}_\mathrm{m}|^2\right)\\&+\left(|\boldsymbol{d}^\mathrm{A}_\mathrm{e}|^2+|\boldsymbol{d}^\mathrm{A}_\mathrm{m}|^2\right)\left(|\boldsymbol{d}^\mathrm{D}_\mathrm{e}|^2+|\boldsymbol{d}^\mathrm{D}_\mathrm{m}|^2\right)\left[\frac{\omega^2r^2}{c^2}+\frac{\omega^4r^4}{c^4}\right]\Bigg\}.\end{aligned} \tag{37}$$

Dividing them by each other and approximating $|\boldsymbol{d}_\mathrm{e}|\gg|\boldsymbol{d}_\mathrm{m}|$ for all molecules leads then to the degree of discrimination given by equation (49).

4.2. RET rate in chiral medium

When donor and acceptor are immersed in a chiral medium, we use the local-field corrected chiral bulk Green's tensor (21) to evaluate the rate formula (5). The two discriminatory and one nondiscriminatory contributions to the rate in terms of dual rate terms (6) are given by

$$\Gamma^\mathrm{D}_\mathrm{disc}=\Gamma_\mathrm{emme}+\Gamma_\mathrm{emem}+\Gamma_\mathrm{meme}+\Gamma_\mathrm{meem}\propto R_\mathrm{D}R_\mathrm{A}, \tag{38}$$

$$\Gamma^\chi_\mathrm{disc}=\Gamma_\mathrm{emee}+\Gamma_\mathrm{meee}+\Gamma_\mathrm{emmm}+\Gamma_\mathrm{memm}\propto R_\mathrm{A}\chi, \tag{39}$$

$$\Gamma_\mathrm{nd}=\sum_{\lambda\lambda'}\Gamma_{\lambda\lambda\lambda'\lambda'}. \tag{40}$$

We refrain from giving their explicit forms, as these expressions are very lengthy and convoluted.

4.3. RET rate in the presence of a chiral mediator

Using the general rate equation (5) together with the Green's tensor given by equation (28), we can calculate the RET rate in the presence of a chiral mediator. The total rate can be divided into three different parts, such that

$$\Gamma=\Gamma_\mathrm{DA}+\Gamma_\mathrm{DA-DMA}+\Gamma_\mathrm{DMA}, \tag{41}$$

$$\Gamma_\mathrm{DA}=\sum\Gamma_{\lambda_1\lambda_2\lambda_3\lambda_4}, \tag{42}$$

$$\Gamma_\mathrm{DA-DMA}=\sum\Gamma^{\lambda_a\lambda_b}_{\lambda_1\lambda_2\lambda_3\lambda_4}, \tag{43}$$

$$\Gamma_\mathrm{DMA}=\sum\Gamma^{\lambda_a\lambda_b\lambda_c\lambda_d}_{\lambda_1\lambda_2\lambda_3\lambda_4}, \tag{44}$$

where Γ_DA and Γ_DMA are the rates from direct and mediated transfer, respectively, and $\Gamma_\mathrm{DA-DMA}$ is their interference term. The individual contributions are given by equation (6) and additionally

$$\Gamma^{\lambda_a\lambda_b}_{\lambda_1\lambda_2\lambda_3\lambda_4} = \frac{2\pi\rho\mu_0^2}{9\hbar^2}\left(\boldsymbol{d}^{\mathrm{A}}_{\lambda_1}\cdot\boldsymbol{d}^{\mathrm{A}*}_{\lambda_2}\right)\left(\boldsymbol{d}^{\mathrm{D}*}_{\lambda_3}\cdot\boldsymbol{d}^{\mathrm{D}}_{\lambda_4}\right)\alpha_{\lambda_a\lambda_b} \times \mathrm{Tr}\left[\mathbb{G}^{(0)}_{\lambda_1\lambda_4}(\boldsymbol{r}_{\mathrm{A}},\boldsymbol{r}_{\mathrm{D}})\cdot\mathbb{G}^{(0)*T}_{\lambda_a\lambda_3}(\boldsymbol{r}_{\mathrm{M}},\boldsymbol{r}_{\mathrm{D}})\cdot\mathbb{G}^{(0)*T}_{\lambda_2\lambda_b}(\boldsymbol{r}_{\mathrm{A}},\boldsymbol{r}_{\mathrm{M}})\right] + \mathrm{c.c.}\,, \tag{45}$$

$$\Gamma^{\lambda_a\lambda_b\lambda_c\lambda_d}_{\lambda_1\lambda_2\lambda_3\lambda_4} = \frac{2\pi\rho\mu_0^2}{9\hbar^2}\left(\boldsymbol{d}^{\mathrm{A}}_{\lambda_1}\cdot\boldsymbol{d}^{\mathrm{A}*}_{\lambda_2}\right)\left(\boldsymbol{d}^{\mathrm{D}*}_{\lambda_3}\cdot\boldsymbol{d}^{\mathrm{D}}_{\lambda_4}\right)\alpha_{\lambda_a\lambda_b}\alpha_{\lambda_c\lambda_d} \times \mathrm{Tr}\left[\mathbb{G}^{(0)}_{\lambda_1\lambda_d}(\boldsymbol{r}_{\mathrm{A}},\boldsymbol{r}_{\mathrm{M}})\cdot\mathbb{G}^{(0)}_{\lambda_c\lambda_4}(\boldsymbol{r}_{\mathrm{M}},\boldsymbol{r}_{\mathrm{D}})\cdot\mathbb{G}^{(0)*T}_{\lambda_a\lambda_3}(\boldsymbol{r}_{\mathrm{M}},\boldsymbol{r}_{\mathrm{D}})\cdot\mathbb{G}^{(0)*T}_{\lambda_2\lambda_b}(\boldsymbol{r}_{\mathrm{A}},\boldsymbol{r}_{\mathrm{M}})\right]. \tag{46}$$

In the case of an unknown acceptor enantiomer we hence obtain two different discriminatory rates, one where the donor discriminates the acceptor $\Gamma^{\mathrm{D}}_{\mathrm{disc}} \propto R_{\mathrm{A}}R_{\mathrm{D}}$ and one where the mediator discriminates the acceptor $\Gamma^{\mathrm{M}}_{\mathrm{disc}} \propto R_{\mathrm{A}}R_{\mathrm{M}}$. They are given by

$$\begin{aligned}\Gamma^{\mathrm{D}}_{\mathrm{disc}} = \sum\Big[&\Gamma_{\mathrm{emem}} + \Gamma_{\mathrm{meem}} + \Gamma_{\mathrm{meme}} + \Gamma_{\mathrm{emme}} \\ &+ \Gamma^{\lambda\lambda}_{\mathrm{emem}} + \Gamma^{\lambda\lambda}_{\mathrm{meem}} + \Gamma^{\lambda\lambda}_{\mathrm{meme}} + \Gamma^{\lambda\lambda}_{\mathrm{emme}} \\ &+ \Gamma^{\lambda\lambda\lambda'\lambda'}_{\mathrm{emem}} + \Gamma^{\lambda\lambda\lambda'\lambda'}_{\mathrm{meem}} + \Gamma^{\lambda\lambda\lambda'\lambda'}_{\mathrm{meme}} + \Gamma^{\lambda\lambda\lambda'\lambda'}_{\mathrm{emme}} \\ &+ \Gamma^{\lambda_1\lambda_2\lambda_1\lambda_2}_{\mathrm{meme}} + \Gamma^{\lambda_1\lambda_2\lambda_2\lambda_1}_{\mathrm{emme}}\Big] \\ \propto\, & R_{\mathrm{A}}R_{\mathrm{D}}\,,\end{aligned} \tag{47}$$

with $\lambda_1 \neq \lambda_2$ and,

$$\begin{aligned}\Gamma^{\mathrm{M}}_{\mathrm{disc}} = \sum\Big[&\Gamma^{\mathrm{em}}_{\mathrm{em}\lambda\lambda} + \Gamma^{\mathrm{me}}_{\mathrm{em}\lambda\lambda} + \Gamma^{\mathrm{em}}_{\mathrm{me}\lambda\lambda} + \Gamma^{\mathrm{me}}_{\mathrm{me}\lambda\lambda} \\ &+ \Gamma^{\mathrm{em}\lambda'\lambda'}_{\mathrm{em}\lambda\lambda} + \Gamma^{\mathrm{me}\lambda'\lambda'}_{\mathrm{em}\lambda\lambda} + \Gamma^{\mathrm{em}\lambda'\lambda'}_{\mathrm{me}\lambda\lambda} + \Gamma^{\mathrm{me}\lambda'\lambda'}_{\mathrm{me}\lambda\lambda} \\ &+ \Gamma^{\lambda'\lambda'\mathrm{em}}_{\mathrm{em}\lambda\lambda} + \Gamma^{\lambda'\lambda'\mathrm{me}}_{\mathrm{em}\lambda\lambda} + \Gamma^{\lambda'\lambda'\mathrm{em}}_{\mathrm{me}\lambda\lambda} + \Gamma^{\lambda'\lambda'\mathrm{me}}_{\mathrm{me}\lambda\lambda}\Big] \\ \propto\, & R_{\mathrm{A}}R_{\mathrm{M}}\,.\end{aligned} \tag{48}$$

The remaining nonvanishing contributions form the nondiscriminatory rate Γ_{nd}. Similar to the chiral medium case, we refrain from giving their explicit form, as these expressions are very lengthy and convoluted.

The chosen simplifying assumptions of isotropic mediator transitions, resonance and lastly that all three involved molecules are of the same species enable us to discuss the degree of discrimination in the presence of the mediator independent of the molecular-species. Relaxing any of these assumptions for the application to different systems is however straightforward.

5. Degree of discrimination

We derived the RET rate Γ (5) between a chiral excited donor molecule and a chiral ground-state acceptor molecule by using perturbation theory within macroscopic QED [32]. We may then take the environment of interest (here free space, chiral medium and a chiral mediator molecule in resonance) into account by substituting the appropriate Green's tensor into equation (6). The resulting rate then consists of a contribution Γ_{nd} insensitive to the handedness of the acceptor and contributions Γ_{disc} sensitive to the acceptor's handedness. Depending on the system the discriminatory contribution itself may consist of several parts that either arise from the chirality of the donor, the chirality of the medium or the chirality of the mediator.

We defined the degree of discrimination as $\delta = \Gamma_{\mathrm{disc}}/\Gamma_{\mathrm{nd}}$ (12). By using equations (36) and (37) we obtain for δ in free space,

$$\delta_0 = \frac{R_{\mathrm{A}}R_{\mathrm{D}}}{c^2|\boldsymbol{d}^{\mathrm{A}}_{\mathrm{e}}|^2|\boldsymbol{d}^{\mathrm{D}}_{\mathrm{e}}|^2}\frac{\left(3c^4+2c^2r^2\omega^2+2r^4\omega^4\right)}{\left(3c^4+c^2r^2\omega^2+r^4\omega^4\right)}\,, \tag{49}$$

where r is the intermolecular distance and $\hbar\omega$ is the transition energy, and we have approximated $|\boldsymbol{d}_{\mathrm{e}}| \ll |\boldsymbol{d}_{\mathrm{m}}|$ to simplify the expression. The degree of discrimination assumes lower and upper bounds in the limit of very small, nonretarded distances $\omega r/c \ll 1$, and very large, retarded distances $\omega r/c \gg 1$, compared to the reduced wavelength $\lambda = c/\omega$ of the dominant molecular transition respectively. In the limit of small distances we find

$$\lim_{r\to 0}\delta_0 = \frac{R_{\mathrm{A}}R_{\mathrm{D}}}{c^2|\boldsymbol{d}^{\mathrm{A}}_{\mathrm{e}}|^2|\boldsymbol{d}^{\mathrm{D}}_{\mathrm{e}}|^2}\,, \tag{50}$$

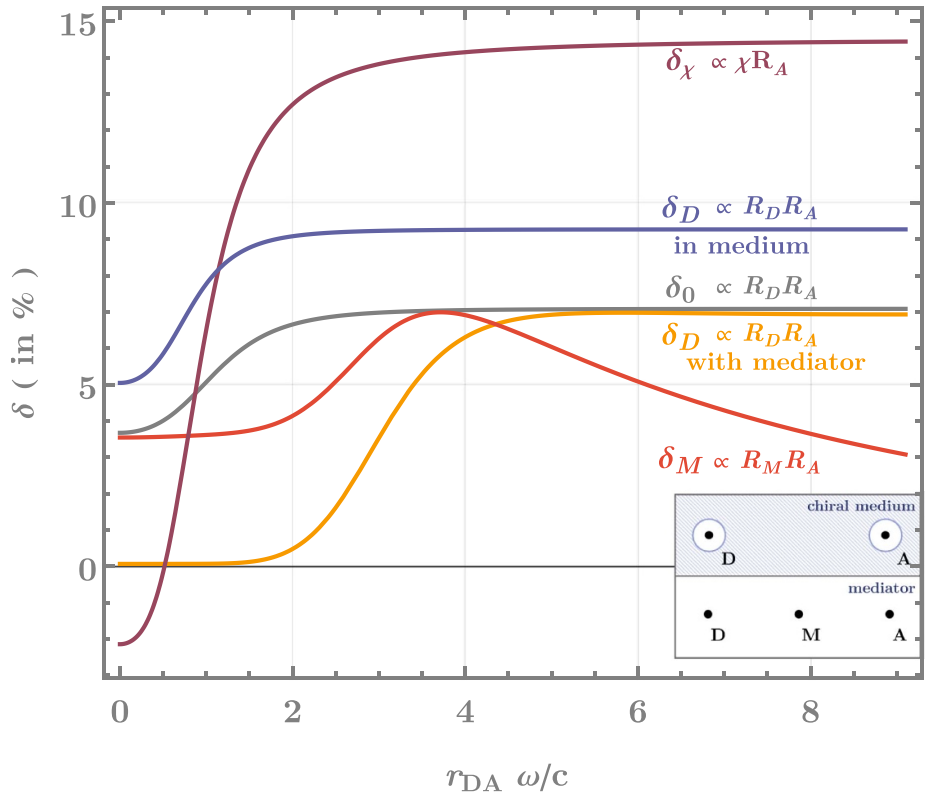

Figure 2. Degree of discrimination δ for the example of 3-MCP for all cases presented in this work: the free space degree of discrimination δ_0, the discrimination due to the chirality of a chiral medium δ_χ, the discrimination due to the donor inside a chiral medium δ_D, the discrimination due to a chiral mediator in the center between donor and acceptor δ_M and the discrimination due to the donor with a mediator between donor and acceptor δ_D.

while the upper (retarded or far-zone) limit is given by approximately twice the lower limit. The degree of discrimination as a function of the distance r is plotted in figure 2 in comparison with the cases considered in the following for the example of 3-methyl-cyclopentanone (3-MCP) as donor and acceptor species.

For the comparison of the discrimination in all presented cases in figure 2, we have chosen 3-MCP in its equatorial methyl-group configuration. 3-MCP in this configuration features a transition with a very small electric transition dipole moment ($|\boldsymbol{d}_\mathrm{e}| = 2.44 \times 10^{-31}$ Cm) compared to its magnetic one ($|\boldsymbol{d}_\mathrm{m}| = 3.31 \times 10^{-32}$ Cm) [41–44]. This leads to a relatively large rotatory strength $R/c = \mathrm{Im}[\boldsymbol{d}_\mathrm{e} \cdot \boldsymbol{d}_\mathrm{m}] \approx |\boldsymbol{d}_\mathrm{e}|^2/7$. The transition energy is given by $\hbar\omega = 4.23$ eV (6.44×10^{15} s^{-1}) and a reduced transition wavelength of $c/\omega = \lambda/2\pi = 46.87$ nm. The chosen example is a chiral molecule whose properties are well known and which has been used in a variety of similar studies with the aim of achieving discrimination such as in [44]. This makes 3-MCP an appropriate candidate system to demonstrate the discriminatory power of RET.

Employing the framework of macroscopic QED allows us to account for the impact of a chiral environment on the process rate by determining the appropriate classical Green's tensor $\mathbb{G}$ that solves the Helmholtz equation and its boundary conditions in the presence of the environment of interest.

We first consider a chiral medium surrounding the molecular system as depicted in figure 1(b). The chiral medium may be characterized by its permittivity ε, permeability μ and its chirality χ. The sign of χ then depends on the handedness of the medium. In the case of a medium surrounding the system, local-field and screening effects must be accounted for via LFCs. Here, we chose the Onsager real cavity model to calculate the LFC for the Green's tensor inside a chiral medium. The resulting corrections to the Green's tensor are much more involved than the ones obtained inside a nonchiral one. While for a nonchiral medium one finds two different correction factors $c_\mathrm{e} = 3\varepsilon/(1+\varepsilon)$ and $c_\mathrm{m} = 3/(1+2\mu)$ for electric and magnetic interactions, the chiral LFC leads to four different correction factors that additionally distinguish between left- and right-handed circularly polarised (L- and R-HCP) excitations of the electromagnetic field. In the first order of the medium chirality, χ they are given by equations (24) and (25), $c_{\mathrm{eL/R}} \approx c_\mathrm{e} \mp \chi\zeta_\mathrm{e}$, $c_{\mathrm{mL/R}} \approx c_\mathrm{m} \pm \chi\zeta_\mathrm{m}$, where c_e and c_m are the known electric and magnetic correction factors for a nonchiral medium and the additional chiral contributions to the correction factors are given by $\zeta_\mathrm{e} = \zeta_\mathrm{m}/2 = c_\mathrm{e}c_\mathrm{m}/3\sqrt{\varepsilon\mu}$. The local-field corrected Green's tensor for a chiral bulk medium is then given by equation (21).

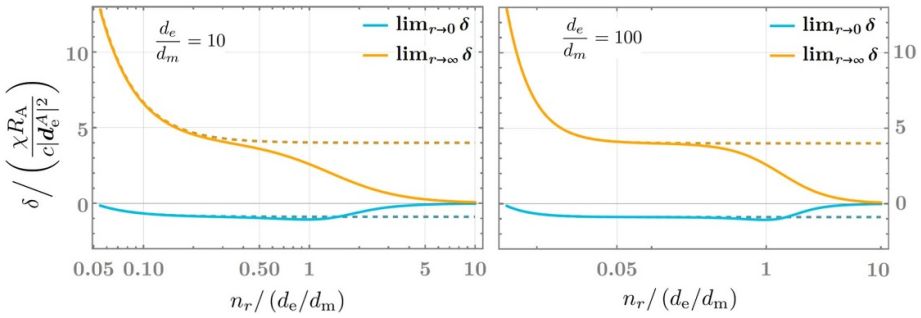

Figure 3. Degree of discrimination due to a surrounding chiral medium in the nonretarded and retarded limits. We have assumed here that the donor and acceptor are the same species. The solid lines are given by the full expression, while the dashed lines are given by the approximations f_0 (54) and f_∞ (55) which are valid for $n_r = \sqrt{\varepsilon\mu} \ll |\boldsymbol{d}_e|/|\boldsymbol{d}_m|$ and we have chosen a trivial permeability $\mu = 1$.

Using the local-field corrected Green's tensor we find that immersed in a chiral medium with known handedness, the total RET rate (5) between a chiral donor with known handedness and a chiral acceptor with unknown handedness features an additional discriminatory contribution,

$$\Gamma = \Gamma_{\mathrm{nd}} + \Gamma^{\mathrm{D}}_{\mathrm{disc}} + \Gamma^{\chi}_{\mathrm{disc}}\,, \tag{51}$$

where similar to the free-space case $\Gamma^{\mathrm{D}}_{\mathrm{disc}} \propto R_{\mathrm{A}} R_{\mathrm{D}}$, but we also find the contribution $\Gamma^{\chi}_{\mathrm{disc}} \propto R_{\mathrm{A}}\chi$. Analogously, the degree of discrimination inside a chiral medium can be split into two terms, such that

$$\delta = \delta_{\mathrm{D}} + \delta_{\chi}\,, \tag{52}$$

where $\delta_{\mathrm{D}} = \Gamma^{\mathrm{D}}_{\mathrm{disc}}/\Gamma_{\mathrm{nd}}$ is the donor-induced degree of discrimination and $\delta_{\chi} = \Gamma^{\chi}_{\mathrm{disc}}/\Gamma_{\mathrm{nd}}$ the medium-induced degree of discrimination.

In the first order of the medium chirality $\chi \ll 1$, the donor-induced degree of discrimination δ_{D} yields the same result as that obtained inside a nonchiral medium [1].

In this work, we focus on the discrimination of the acceptor that arises from the medium, δ_{χ}. Similar to the free-space case we find that δ_{χ} assumes lower and upper bounds in the two opposite distance limits. Assuming $|n_r \boldsymbol{d}_{\mathrm{m}}| \ll |\boldsymbol{d}_{\mathrm{e}}|$ and $\chi \ll 1$, they can be approximated by

$$\lim_{r\to 0}\delta_{\chi} \approx \frac{\chi R_{\mathrm{A}}}{c|\boldsymbol{d}_{\mathrm{e}}^{\mathrm{A}}|^2} \times f_0\,, \qquad \lim_{r\to\infty}\delta_{\chi} \approx \frac{\chi R_{\mathrm{A}}}{c|\boldsymbol{d}_{\mathrm{e}}^{\mathrm{A}}|^2} \times f_\infty\,, \tag{53}$$

with f_0 and f_∞ entirely determined by the properties of the medium,

$$f_0 = \frac{2n_r\left(c_{\mathrm{m}}\zeta_{\mathrm{e}} - c_{\mathrm{e}}\zeta_{\mathrm{m}}\right)}{c_{\mathrm{e}}^2}\,, \tag{54}$$

$$f_\infty = \frac{2\left(3c_{\mathrm{e}}c_{\mathrm{m}} - n_r c_{\mathrm{e}}\zeta_{\mathrm{m}} + 3n_r c_{\mathrm{m}}\zeta_{\mathrm{e}}\right)}{c_{\mathrm{e}}^2}\,, \tag{55}$$

where $n_r = \sqrt{\varepsilon\mu}$ is the nonchiral refractive index, c_λ and ζ_λ are the correction factors, see equations (26) and (27), and we have assumed real valued medium parameters for simplicity.

When neglecting the chirality of the LFC factors in equations (27), i.e. for $\zeta_\lambda = 0$, the medium-induced discrimination vanishes in the limit of small distances, $\lim_{r\to 0}\delta_{\chi} = 0$. The discrimination in this limit is hence entirely due to local-field effects.

Using the explicit expressions for the correction factors given by equations (26) and (27) we find that for media with $|n_r| > 1/2$, which is true for most media, $f_0 < 0$ while $f_\infty > 0$. This is illustrated in figure 3, where f_0 and f_∞ are plotted as a function of the nonchiral refractive index $n_r = \sqrt{\varepsilon\mu}$ (with real permittivities ε and trivial permeability $\mu = 1$).

For the plot, we assumed that donor and acceptor are the same species, where in one case we assume for the transition dipoles $|\boldsymbol{d}_{\mathrm{e}}|/|\boldsymbol{d}_{\mathrm{m}}| = 10$ and in the other $|\boldsymbol{d}_{\mathrm{e}}|/|\boldsymbol{d}_{\mathrm{m}}| = 100$. The behaviour of the bounds for large n_r is determined by $|\boldsymbol{d}_{\mathrm{e}}|/|\boldsymbol{d}_{\mathrm{m}}|$, while the behaviour for small n_r is determined by χ of the medium which we chose here to be 0.3. Furthermore, we find that for real medium properties ε and μ the values of f_0 and f_∞ are given by approximately -1 and 4 for $\chi \ll n_r \ll |\boldsymbol{d}_{\mathrm{e}}|/|\boldsymbol{d}_{\mathrm{m}}|$. As a consequence δ_{χ} changes sign as a function of the intermolecular distance, i.e. while same-handed acceptors are preferred by RET for large distances $r \geqslant c/\omega$, the rate involving opposite-handed acceptors is dominant for small distance $r < c/\omega$.

This is shown for the example of 3-MCP inside a chiral medium with $\chi = 0.3$, $\varepsilon = 1.8$ and $\mu \approx 1$ in figure 2, where δ_χ is plotted as a function of the intermolecular distance in comparison with the remaining cases discussed in this work. An inversion of discrimination as a function of the distance has previously been predicted for strongly absorbing dielectric media surrounding the system [1].

In the limit of a dilute gas as chiral medium, the surrounding environment can alternatively be modelled by N mediator molecules. Electric mediators can be treated as environment by including them into the Green's tensor via their electric polarisability [20–22, 40]. Here, we use such an approach for chiral mediator molecules. The considered system is schematically shown in figure 1(c). We assume that the mediator is possibly a chiral molecule in its ground state that features a resonance for a chiral transition at the exchanged energy $\hbar\omega$.

Similar to the chiral medium, the chiral mediator can itself discriminate the acceptors, assuming that the handedness of the mediator is known. We then find an additional contribution to the degree of discrimination,

$$\delta = \delta_\mathrm{D} + \delta_\mathrm{M}\,, \tag{56}$$

where $\delta_\mathrm{D} \propto R_\mathrm{A} R_\mathrm{D}$ is the donor-induced degree of discrimination, and $\delta_\mathrm{M} \propto R_\mathrm{A} R_\mathrm{M}$ is the mediator-induced degree of discrimination whose rotatory strength is R_M.

The rate Γ in the presence of a mediator in lowest-order perturbation theory consists of three parts, where one term results from the direct transfer of the excitation from donor to acceptor independent of the mediator, Γ_DA, one part from the scattering of the excitation at the mediator, Γ_DMA, and lastly one term from the interference of both process paths, $\Gamma_\mathrm{DA-DMA}$. In the nonretarded or near-zone limit $\omega r/c \ll 1$, the mediated transfer rate Γ_DMA dominates the RET rate; assuming that $|\boldsymbol{d}_\mathrm{e}| \gg |\boldsymbol{d}_\mathrm{m}|$ for all involved molecules, we find

$$\lim_{r\to 0}\delta \approx \lim_{r\to 0}\delta_\mathrm{M} = \frac{R_\mathrm{A} R_\mathrm{M}}{c^2 |\boldsymbol{d}_\mathrm{e}^\mathrm{A}|^2 |\boldsymbol{d}_\mathrm{e}^\mathrm{M}|^2}\,, \tag{57}$$

where $\boldsymbol{d}_\mathrm{e}^\mathrm{M}$ is the electric transition dipole moment of the mediator. The degree of discrimination in this limit is hence comparable to the one found in free space, equation (50). While the discrimination in this limit does not change significantly, the RET rate itself can be greatly enhanced in the presence of a close-by mediator [20–22]. In the case of an achiral mediator, i.e. $R_\mathrm{M} = 0$, the mediation even leads to a suppression of the discrimination by a factor of $|\boldsymbol{d}_\mathrm{m}^\mathrm{M}|^2/|\boldsymbol{d}_\mathrm{e}^\mathrm{M}|^2 \ll 1$ compared to the nonretarded discrimination in free space. In this case we find

$$\lim_{r\to 0}\delta = \lim_{r\to 0}\delta_\mathrm{D} \approx \frac{|\boldsymbol{d}_\mathrm{m}^\mathrm{M}|^2}{|\boldsymbol{d}_\mathrm{e}^\mathrm{M}|^2} \times \frac{R_\mathrm{A} R_\mathrm{D}}{c^2 |\boldsymbol{d}_\mathrm{e}^\mathrm{A}|^2 |\boldsymbol{d}_\mathrm{e}^\mathrm{D}|^2}\,. \tag{58}$$

In the opposite distance limit $\omega r/c \gg 1$, the transfer rate is dominated by the direct transfer Γ_DA and is independent of the mediator. The degree of discrimination is hence given by the free space result (49) in the retarded or far-zone distance limit.

In the intermediate distance regime, the relative positions of the three particles can have a large impact on the discriminatory effect. This is shown in figures 4 and 5 for the nonretarded and retarded regime, respectively. We assume for the plots that all three particles are the same species, where the mediator and donor are same-handed and their handedness is known. We have normalised the results to the free-space case, which due to the assumption $|\boldsymbol{d}_\mathrm{e}| \gg |\boldsymbol{d}_\mathrm{m}|$ yields molecule-independent results.

In figure 4 the degree of discrimination is plotted when the donor and acceptor molecules are placed at a nonretarded distance of $r_\mathrm{DA}\omega/c = 0.2$ and the mediator position is varied. Placing the mediator in the center of the donor and acceptor suppresses the donor-induced discrimination, $\delta_\mathrm{D} \approx 0$, but shows the highest discriminatory effect via the mediator, which is comparable to the free space discrimination, $\delta_\mathrm{M} \sim \delta_0$. Placing the donor further from the center inverts this scenario, such that $\delta_\mathrm{M} \approx 0$ and $\delta_\mathrm{D} \approx \delta_0$. As a consequence, the combined discrimination $\delta = \delta_\mathrm{M} + \delta_\mathrm{D}$ is approximately position-independent and comparable to the free space discrimination δ_0.

In figure 5 the degree of discrimination is plotted when the donor and acceptor molecules are placed at a retarded distance of $r_\mathrm{DA}\omega/c = 5$ and the mediator position is varied. The mediator-induced discrimination δ_M is again largest and comparable to the free space discrimination δ_0 when placing the mediator at the center of the geometry, while the donor-induced discrimination δ_D is best enhanced by the mediator by placing it at narrow interference peaks outside the center of the donor-acceptor pair and on their connecting axis. The total discrimination $\delta = \delta_\mathrm{D} + \delta_\mathrm{M}$ then profits most from a mediator placed at the center, where the discrimination can be roughly doubled compared to δ_0.

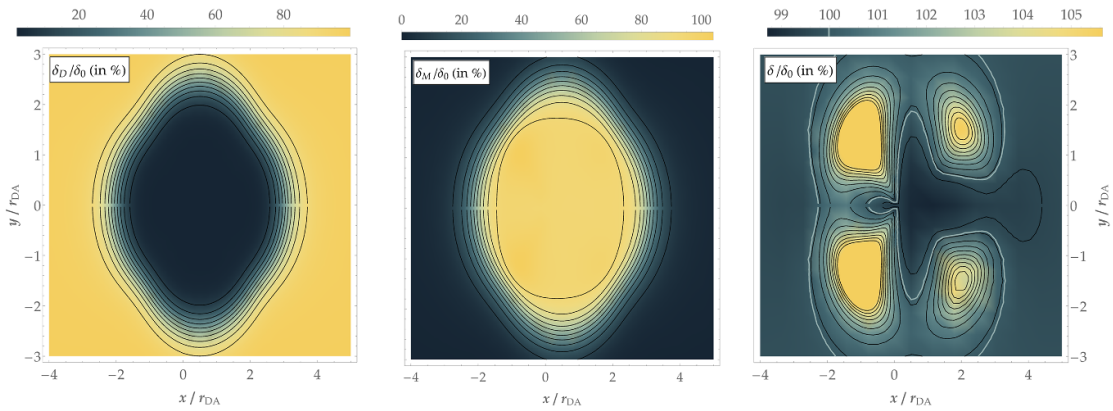

Figure 4. Degree of discrimination in the presence of a mediator in the nonretarded distance regime as a function of the mediator position. We divide the degree of discrimination into two parts, one part arising from the chiral property of the mediator δ_{M} and one from the chiral property of the donor δ_{D}, see equation (56), while the total degree of discrimination is given by their sum $\delta = \delta_{\mathrm{D}} + \delta_{\mathrm{M}}$. The donor is placed at the origin $(0, 0)$, while the acceptor is placed at $(r_{\mathrm{DA}}, 0)$ with a nonretarded distance $r_{\mathrm{DA}} = 0.2c/\omega$ from the donor. We assume here that all three particles are the same species.

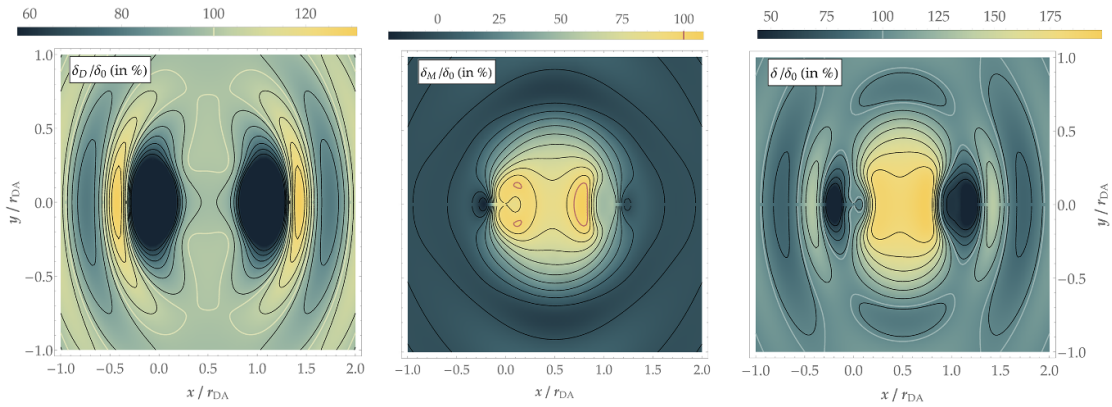

Figure 5. Degree of discrimination in the presence of a mediator in the retarded distance regime as a function of the mediator position. We divide the degree of discrimination into two parts, one part arising from the chiral property of the mediator δ_{M} and one from the chiral property of the donor δ_{D}, see equation (56), while the total degree of discrimination is given by their sum $\delta = \delta_{\mathrm{D}} + \delta_{\mathrm{M}}$. The donor is placed at the origin $(0, 0)$, while the acceptor is placed at $(r_{\mathrm{DA}}, 0)$ with a retarded distance $r_{\mathrm{DA}} = 5c/\omega$ from the donor. We assume here that all three particles are the same species.

The discrimination in the presence of a mediator is additionally plotted as a function of the donor–acceptor-distance for the example of all three molecules being 3-MCP in figure 2 in comparison with the discrimination inside a chiral medium and the free-space case. The mediator is here fixed at the center point between the donor and acceptor. The plot also shows the discussed distance limits for δ_{D} and δ_{M}.

The analysis assumes that the positions of the involved molecules is known. In real-life applications this will not be the case. In case of densities of molecule clouds the positions need to be integrated over. For acceptor and donor clouds (assuming that the donors are prepared in an incoherent initial state) the integration over the densities is performed over the rates itself. In case of the mediator cloud the integration has to be done over the transition matrix element M_{fi}, which could in general lead to new interference features but will usually *wash out* the interference patterns shown in figures 4 and 5. While the microscopic picture is of course related to the macroscopic one, the results seem fundamentally different. This is due to our assumption in the microscopic case of being on resonance with the transition in the mediator molecule which we assume to have a narrow width that is given by the spontaneous decay rate.

6. Conclusion

In this study we have examined discrimination through RET involving chiral molecules within a chiral environment; we have focused on attempting to discriminate between differently handed acceptor particles. Our investigation involved two different chiral environments: a macroscopic chiral medium surrounding both the donor and acceptor molecules, and a single chiral mediator molecule in close proximity.

By applying the Curie symmetry principle to the challenge of chiral discrimination, it becomes evident that detecting the handedness of a given chiral object necessitates the incorporation of the handedness of another chiral object. Consequently, our findings underscore the necessity of introducing a chiral element with a predetermined handedness to elicit the discriminatory effect. This chiral element can manifest as the donor molecule itself, the surrounding medium, or the mediator molecule. The resulting discrimination can then be categorized as arising either from the donor (δ_{D}), the mediator (δ_{M}) or the medium (δ_{χ}). Furthermore, an implication of the Curie symmetry principle is the absence of a three-body discrimination scenario, exemplified by a rate contribution proportional to $R_{\mathrm{A}}R_{\mathrm{D}}R_{\mathrm{M}}$ in the mediator case or $R_{\mathrm{A}}R_{\mathrm{D}}\chi$ in the medium case. We may prove this by contradiction: let us suppose that contributions proportional to $R_{\mathrm{A}}R_{\mathrm{D}}R_{\mathrm{M}}$ persist and that we lack prior knowledge of the participants' handedness. This would lead to the left-handed molecule-specific rate Γ_{LLL} featuring a positive term proportional to $R_{\mathrm{A}}R_{\mathrm{D}}R_{\mathrm{M}}$, while Γ_{RRR} would exhibit the same term but with an opposite sign. Consequently, one could potentially measure $\Gamma_{\mathrm{LLL}} > \Gamma_{\mathrm{RRR}}$, thereby distinguishing these scenarios without any prior knowledge of handedness. Given that such a situation contradicts the Curie symmetry principle, we infer that these contributions must indeed vanish across all systems.

We proceeded to analyze the discrimination attributed to a chiral medium, denoted as δ_{χ}, revealing that for the majority of systems, discrimination in the retarded (far-zone) limit is approximated as $\delta_{\chi} \approx 4\chi R_{\mathrm{A}}/(c|\boldsymbol{d}_{\mathrm{e}}^{\mathrm{A}}|^2)$, while in the nonretarded (near-zone) limit, we obtain $\delta_{\chi} \approx -\chi R_{\mathrm{A}}/(c|\boldsymbol{d}_{\mathrm{e}}^{\mathrm{A}}|^2)$. These approximations are applicable to systems satisfying the conditions $\chi \ll 1$, $|\boldsymbol{d}_{\mathrm{m}}| \ll |\boldsymbol{d}_{\mathrm{e}}|$, $\mu - 1 \ll 1$, and $\chi \ll n_r \ll |\boldsymbol{d}_{\mathrm{e}}|/|\boldsymbol{d}_{\mathrm{m}}|$. Notably, the alteration in the sign of δ_{χ} concerning distance implies a shift in the preferred handedness for RET discrimination as the distance changes.

This inversion of discrimination emerges as a direct consequence of the introduced LFCs. Our approach involved the formulation of a LFC model designed for chiral media, built upon the Onsager real cavity model. In this model, infinitesimally small vacuum spheres encompassing both the donor and acceptor positions are introduced. Within this configuration, the Green's tensor, which characterizes the excitation transfer from donor to acceptor, comprises two transmissions through the surfaces of these vacuum spheres. We expressed these transmissions as matrices operating within a selected spherical vector wave function framework, akin to the well-established approach for planar multilayered systems [45]. Specifically, as the sphere radius becomes infinitesimally small, these transmission matrices can be approximated by diagonal matrices, ultimately yielding the correction factors (as detailed in equation (27) that are subsequently applied to the chiral bulk Green's tensor (as shown in equation (21)). This corrected chiral bulk Green's tensor offers a versatile tool for investigating various processes immersed within a chiral medium.

The distance at which inversion can be observed is in the nonretarded regime and as such is notably small. In the illustrated case of 3-MCP, we anticipate the inversion to transpire around $r \approx 0.5c/\omega$, corresponding to approximately 25 nm. When distances closely align with the dimensions of the involved molecules, additional effects and processes become relevant, such as Dexter electron transfer. This transfer arises from the electron wave function overlap between the molecules and is expected to emerge over a distance of several Angstrø ms. While it is possible to expand the theory to incorporate Dexter transfer, it is important to recognise that the results would then be heavily reliant on the particular molecular system under consideration, and substantive variations would mainly emerge at distances within the Angstrø m scale. Given that our objective is to gain general insights from an analytical exploration, we have intentionally excluded these effects.

In analogy to their molecular counterparts, namely $\boldsymbol{d}_{\mathrm{e}}$, $\boldsymbol{d}_{\mathrm{m}}$, and R, the properties of the medium, i.e. ε, μ, and χ, are not entirely independent parameters. Consequently, when considering a fixed chirality (χ), the nonchiral refractive index (n_r) cannot be chosen arbitrarily small. Employing a microscopic model for the medium or adopting the Drude–Lorentz model could offer a means to incorporate these interconnected relationships. It is worth noting that we deliberately refrained from selecting parameter combinations for the medium that could potentially contradict these underlying dependencies.

Nevertheless, we have systematically presented our findings across an extensive parameter space of media. The dynamic evolution within the metamaterials realm continually expands our capacity to tailor media with precise optical characteristics. While the domain of metafluids remains in its early stages, the implications of our results extend to solid materials as well, leveraging the extensive spectrum of metamaterials that has been both developed and studied.

It is worth emphasising that the presented results for a system immersed in a chiral medium are valid for macroscopic media whose optical properties are well described by their macroscopic parameters within the relevant length scale. Nonetheless, the assumption of macroscopic parameters might not be adequate for highly dilute gases, where the medium's behavior is primarily governed by its individual constituents. In this context, we probed the impact of a single chiral mediator molecule in the vicinity of the system.

Our findings demonstrate that in the limit of nonretarded distances between molecules, the discrimination is predominantly dictated by the mediator. In stark contrast, at large separation distances, the discrimination becomes independent of the mediator, with the sole contribution originating from the donor particle. Meanwhile, the intermediate distance regime exhibits a pronounced reliance on the specific geometry. For distances smaller than the reduced wavelength, discrimination arises solely from either the mediator or the donor depending on the geometry, with negligible additive effects between the two. In scenarios where the donor and acceptor are separated by several reduced wavelengths, we noted that the mediator-induced discrimination δ_{M} benefits most from a central mediator placement. Conversely, the enhancement of discrimination δ_{D} attributable to the donor occurs most effectively when placing the mediator on interference peaks outside the donor-acceptor arrangement. This nicely illustrates the intricacies that arise on the introduction of a third-body and the roles played by direct, relay, and interference pathways [20–22, 46, 47].

Our approach involved introducing assumptions pertaining to the mediator and its polarizability tensor, enabling a comprehensive discussion that maintains generality. Relaxing these assumptions will lead to results contingent on the mediator's specific molecular structure [28]. Furthermore, our framework can be easily extended to multiple mediators and mediator cloud densities. Multiple mediators introduce additional process channels that interfere with each other, while substituting specific mediator positions with densities results in the blurring of interference patterns.

In summation, we proffer a variety of overarching insights into RET taking place within chiral environments. Our presented results furnish a guiding framework for future explorations in this domain, potentially facilitating intuitive predictions. For tailored systems, precision in calculations can be enhanced through the various methodologies we have discussed. Novel techniques for accommodating chiral environments within the macroscopic QEDs framework have been introduced and elaborated upon. We employed the Onsager real cavity model to account for local-field and screening effects within chiral media, leading to corrections to the rate of energy transfer. As a consequence, our findings reveal an intriguing asymmetry: while one chiral handedness of the acceptor is preferred by the energy transfer in one distance regime, the opposite handedness prevails in the alternate regime. It would be interesting to employ alternative models for LFCs in future work in order to study this asymmetry further. Any proposed or actual experiments may prove involved in trying to measure the effect of the chiral medium relative to discrimination occurring between donor and acceptor moieties, and it is hoped that this work will stimulate further experimental study.

Data availability statement

All data that support the findings of this study are included within the article (and any supplementary files).

Acknowledgment

This work was supported by the German Research Foundation (DFG, Project No. 328961117-SFB 1319 ELCH).

ORCID iDs

Janine C Franz https://orcid.org/0000-0002-5452-8279
A Salam https://orcid.org/0000-0001-5167-4767

References

[1] Franz J C, Buhmann S Y and Salam A 2023 *Phys. Rev.* A **107** 032809
[2] Craig D P and Thirunamachandran T 1998 *J. Chem. Phys.* **109** 1259–63
[3] Salam A 2005 *J. Chem. Phys.* **122** 044113
[4] Salam A 2018 *Atoms* **6** 56
[5] Jones G A and Bradshaw D S 2019 *Front. Phys.* **7** 100
[6] Barron L D 2004 *Molecular Light Scattering and Optical Activity* (Cambridge University Press)
[7] Yoo S and Park Q-H 2015 *Phys. Rev. Lett.* **114** 203003
[8] Baranov D G, Schäfer C and Gorkunov M V 2023 *ACS Photonics* **10** 2440–55
[9] Schäfer C and Baranov D G 2023 *J. Phys. Chem. Lett.* **14** 3777–84
[10] Hübener H, Giovannini U D, Schäfer C, Andberger J, Ruggenthaler M, Faist J and Rubio A 2020 *Nat. Mater.* **20** 438–42
[11] Owens J C, Panetta M G, Saxberg B, Roberts G, Chakram S, Ma R, Vrajitoarea A, Simon J and Schuster D I 2022 *Nat. Phys.* **18** 1048–52
[12] Jenkins J K, Salam A and Thirunamachandran T 1994 *Phys. Rev.* A **50** 4767–77
[13] Salam A 2009 *Molecular Quantum Electrodynamics–Long-Range Intermolecular Interactions* (Wiley)

[14] Safari H, Barcellona P, Buhmann S Y and Salam A 2020 *New J. Phys.* **22** 053049
[15] Ordonez A F and Smirnova O 2018 *Phys. Rev.* A **98** 063428
[16] Domingos S R, Pérez C, Marshall M D, Leung H O and Schnell M 2020 *Chem. Sci.* **11** 10863–70
[17] Ayuso D, Ordonez A F, Ivanov M and Smirnova O 2021 *Optica* **8** 1243
[18] Genet C 2022 *ACS Photonics* **9** 319–32
[19] Guo Y, Gong X, Ma S and Shu C-C 2022 *Phys. Rev.* A **105** 013102
[20] Craig D P and Thirunamachandran T 1989 *Chem. Phys.* **135** 37–48
[21] Daniels G J and Andrews D L 2002 *J. Chem. Phys.* **116** 6701–12
[22] Salam A 2012 *J. Chem. Phys.* **136** 014509
[23] Andrews D L and Ford J S 2013 *J. Chem. Phys.* **139** 014107
[24] Forbes K A, Bradshaw D S and Andrews D L 2019 *J. Chem. Phys.* **151** 034305
[25] Andrews D L 2019 *Methods Appl. Fluorescence* **7** 032001
[26] Salam A 2021 *J. Phys. Chem.* A **125** 3549–55
[27] Salam A 2022 *J. Chem. Phys.* **157** 104110
[28] Salam A 2021 *J. Chem. Phys.* **154** 074111
[29] Onsager L 1936 *J. Am. Chem. Soc.* **58** 1486–93
[30] Buhmann S Y and Welsch D G 2007 *Prog. Quantum Electron.* **31** 51–130
[31] Scheel S and Buhmann S Y 2008 *Acta Phys. Slovaca* **58** 675–809
[32] Buhmann S Y 2012 *Dispersion Forces I – Macroscopic Quantum Electrodynamics and Ground-State Casimir, Casimir–Polder and van der Waals Forces* vol 247 (Springer)
[33] Butcher D T, Buhmann S Y and Scheel S 2012 *New J. Phys.* **14** 113013
[34] Barcellona P, Safari H, Salam A and Buhmann S Y 2017 *Phys. Rev. Lett.* **118** 193401
[35] Andrews D L, Jones G A, Salam A and Woolley R G 2018 *J. Chem. Phys.* **148** 040901
[36] Craig D P and Thirunamachandran T 1992 *Chem. Phys.* **167** 229–40
[37] Juzeliunas G and Andrews D L 2000 *Adv. Chem. Phys.* **112** 357–410
[38] Andrews D L 2008 *Can. J. Chem.* **86** 855
[39] Engheta N and Kowarz M W 1990 *J. Appl. Phys.* **67** 639–47
[40] Waller M C and Bennett R 2022 *Phys. Rev.* A **106** 043107
[41] Kröner D 2011 *J. Phys. Chem.* A **115** 14510–8
[42] Horsch P, Urbasch G, Weitzel K-M and Kröner D 2011 *Phys. Chem. Chem. Phys.* **13** 2378–86
[43] Kröner D 2015 *Phys. Chem. Chem. Phys.* **17** 19643–55
[44] Suzuki F, Momose T and Buhmann S Y 2019 *Phys. Rev.* A **99** 012513
[45] Tomaš M S 1995 *Phys. Rev.* A **51** 2545–59
[46] Ford J S, Salam A and Jones G A 2019 *J. Phys. Chem. Lett.* **10** 5654–61
[47] Green D, Jones G A and Salam A 2020 *J. Chem. Phys.* **153** 034111